LARGE-SIGNAL ANALYSIS OF IN P IMPATT DIODES WITH  
PROPOSED APPLICATIONS TO AIRBORNE-RADAR SYSTEMS

D. Hosny El-Motaafy\* D. M.M.El Arabaty\* Said H.Ebrahim\*

## ABSTRACT

The purpose of this paper is to provide a better understanding of the effects of the operating conditions on the performance of the high efficiency In P-IMPATT diodes. These effects are investigated using the full-scale computer simulation of these devices. The simulation takes fully into account all the physical effects pertinent to the IMPATT diode operation. It is found that by increasing the RF-voltage level across the diode terminals, three different modes of operation can be obtained successively. The first one is the conventional IMPATT mode. The second one is a high-efficiency mode. In this mode, the avalanche-generated pulse (AGP) is bunched and accelerated during the second half cycle causing the induced current  $J_i$  to increase. In the third mode, which is also a high efficiency one, the AGP is prematurely collected. It is found that by increasing the operating frequency, the premature collection of the AGP is either delayed or suppressed but the bunching and acceleration of this pulse become less pronounced. It is found that by increasing the DC-bias current, the premature collection of the AGP is either delayed or suppressed whereas the acceleration and bunching of this pulse are enhanced. On the other hand, the trapping of electrons behind the AGP becomes more significant. It is demonstrated that the optimum values of both the DC-bias current and the RF voltage level increase with the operating frequency. The possible applications of the In P IMPATT diodes to airborne radar systems are indicated.

---

\* Department of Radar (M.T.C.)

## 1- INTRODUCTION

In this paper, a detailed numerical study has been undertaken to get insight into the effects of the operating conditions on the performance of In P IMPATTs. This study has been performed using the full-scale computer simulation program described elsewhere[1]. The IMPATT is assumed to be driven by a terminal voltage  $V_t$  whose DC component is  $V_{dc}$ . The AC component is a sinusoidal voltage of amplitude  $V_{rf}$  and frequency  $F$ . The results presented here are for a n-type LOW-HIGH-LOW diode which has the following structural parameters:

The diode width is  $3.9 \mu\text{m}$ , the avalanche region width is  $0.4 \mu\text{m}$ , the doping density in the avalanche region is  $10^{15} \text{cm}^{-3}$  and in the drift region is  $3 \times 10^{15} \text{cm}^{-3}$ , and the size of the doping clump is  $2.2 \times 10^{12} \text{cm}^{-2}$ .

## 2- THE EFFECTS OF ALTERING THE RF VOLTAGE LEVEL

Figs. 1 and 2 shows the efficiency of the IMPATT versus the RF voltage level  $V_{rf}$  for different values of the DC-bias current density  $J_{dc}$  and the frequency  $F$ . It is seen that there is generally a sudden increase in the efficiency at a certain value of  $V_{rf}$  which changes with both  $J_{dc}$  and  $F$ . This value indicates the onset of the high-efficiency modes as it is indicated elsewhere[2-3]. Fig.3 shows the induced current density  $J_i$  at  $J_{dc}=1200 \text{ A/cm}^2$  and  $F=14 \text{ GHz}$  for different values of  $V_{rf}$ . Fig.4 shows the corresponding spatial distribution of the electron density  $J_n$ . It is clear that at  $V_{rf}=56 \text{ V}$  the diode is operating according to conventional IMPATT mode. The AGP after being injected into the drift region (DR) moves towards the ohmic contact inducing a current in the external circuit in antiphase relationship with the terminal voltage. At a phase angle  $\phi$  of about  $270^\circ$ , the AGP is slightly bunched and accelerated because of the favorable velocity-field characteristics of the In P material. This gives rise to a slight increase of  $J_i$  at this phase angle. This effect becomes more pronounced when  $V_{rf}$  is increased to  $58 \text{ V}$ . At  $V_{rf}=60 \text{ V}$ , the IMPATT is operating according to the second high-mode[2-3] as fig.4 shows. The AGP is significantly bunched and accelerated causing  $J_i$  to undergo a large peak at  $\phi = 270^\circ$ . As  $V_{rf}$  is increased to  $62 \text{ V}$ , the AGP is prematurely collected by the undepleted region which penetrates into the diode. This causes the large dip occurring in  $J_i$  slightly after  $\phi = 270^\circ$  as it is seen in fig. 3-b.

## 3- EFFECTS OF ALTERING THE DC-BIAS CURRENT

Fig.1 shows that when the DC-bias current increases the efficiency decreases slightly and the transition between the conventional IMPATT mode and the high- modes becomes less sharper. Fig.5 through 8 show  $J_i$  and  $J_n$  for  $J_{dc}=1500 \text{ A/cm}^2$  and  $1800 \text{ A/cm}^2$  respectively. By comparing these results with those obtained for  $J_{dc}=1200 \text{ A/cm}^2$ , it is noticed that by increasing  $J_{dc}$  the bunching and acceleration of AGP are enhanced. This improves

6

the performance. On the other hand some electrons are trapped behind the AGP during a small portion of the cycle. These electrons induce local negative currents. This effect slightly degrades the performance. It is also noticed that at  $J_{dc}=1800 \text{ A/cm}^2$ , no premature collection of the AGP occurs. This is because the depletion layer width modulation (DLWM) effect is reduced by increasing  $J_{dc}$ . This means that the ability of the undepleted region to penetrate into the diode is reduced. Consequently the collection of the AGP is either delayed or suppressed

#### 4- THE EFFECTS OF ALTERING THE OPERATION FREQUENCY

Fig.5 shows  $J_i$  at  $J_{dc}=1500 \text{ A/cm}^2$ ,  $V_{rf}=62 \text{ V}$  for  $F=11,12,13$  and  $14 \text{ GHZ}$ . Fig.6 shows  $J_n$  at the same  $J_{dc}$  and  $V_{rf}$  for  $F=12$  and  $13 \text{ GHZ}$ . It is noticed that at  $F=12 \text{ GHZ}$  the AGP is prematurely collected and  $J_i$  undergoes a large dip at  $\phi=270^\circ$ . When  $F$  is increased to  $13 \text{ GHZ}$  the AGP is not collected at all but it continues to be bunched and accelerated. This results can be explained as follows:

As  $F$  is increased, the edge of the depletion layer (EDL) moves more rapidly. Thus the time instant at which the AGP can encounter the EDL is delayed. If  $F$  is increased further, the EDL changes its direction and moves towards the ohmic contact whereas the AGP is still in the middle of the DR. Consequently, the AGP can not be collected by the UDR. It is also noticed that the bunching and acceleration of the AGP become less significant whereas the trapping of electrons behind this AGP is reduced as  $F$  is increased. This is attributed to the decrease of the space charge effect with increasing  $F$ .

Since by decreasing  $V_{rf}$ , the DLWM effect is reduced whereas by decreasing  $J_{dc}$ , the space charge effect becomes less significant, it can be concluded that a slight increase of  $F$  is equivalent to a slight decrease of both  $V_{rf}$  and  $J_{dc}$  fig.2 shows.

#### 5- APPLICATIONS OF IN P IMPATT DIODE TO AIRBORNE RADAR SYSTEMS

The In P IMPATT diode can have many wide applications in airborne multi-function radars, in radar altimeters, in solid-state doppler radars, in electronic scanning radars, and in airborne electronic-counter-measures equipments specially as the active element in barrage jammers.

Fig.9 shows a block diagram of a solid-state X-band doppler radar using the In P IMPATT diode

The In P IMPATT oscillator operates at X-band frequency with bias current regulator. The output power of the IMPATT oscillator is about 10 watts. The isolator is used to protect the IMPATT source from the reflected signals. The mixer is a silicon Schottky barrier diode. The circulator has a dual purpose of

separating the transmitted and received signals, also to get a small fraction of signal power to be used as a local oscillator signal for the mixer. The combiner is used to increase the level of the output power.

Fig.10 shows a block diagram of a solid-state X-band coherent airborne radar transmitter. The IMPATT can be used either a coherent power source or a non-coherent power source. In the non-coherent mode, the IMPATT and its associating circuit operate as a free-running pulsed oscillator with a controlled interpulse thermal frequency chirp. In the coherent mode the IMPATT oscillator is used as the final power amplifier driven by a low noise stable master oscillator (STAM) and operates in the injection locked oscillator (ILO). The stable-master oscillator consists of VHF crystal controlled reference followed by two phased-locked oscillators (PLO) which provide amplification and frequency multiplication. The phase-locked system is a two-loop system. A reference oscillator (supplied from a low FM noise crystal-controlled oscillator) is used to phase-lock a transistor oscillator which provides LO power for mixer. The resultant error signal (output of the detector) is amplified and applied to the GUNN oscillator. The GUNN PLO locks a CW IMPATT oscillator. In the coherent mode the CW ILO locks a pulsed IMPATT oscillator. The IMPATT oscillator exhibits a linear frequency chirp across the pulse.

#### 6- CONCLUSIONS

From the previous analysis it is concluded that the different modes of operation of In P IMPATTs can be obtained successively by increasing  $V_{rf}$ . The efficiencies obtained can exceed 35% at frequencies ranging from 10 to 14 GHz. It is noticed that by increasing the DC-bias current the space charge effect is increased and the DLWM effect is reduced. Consequently the collection of the AGP will be either delayed or suppressed. The bunching and acceleration of the AGP will be enhanced. On the other hand the trapping of the electrons behind the AGP becomes more pronounced. It is demonstrated that by increasing the operating frequency the space charge effect and the DLWM effect are reduced. The AGP will not be sufficiently bunched and accelerated. Furthermore it will not be collected at the proper phase angle. It is concluded that the effects of increasing the operating frequency are similar to those of reducing the RF voltage level and the DC-bias current. Finally the application of In P IMPATT in airborne radar systems are indicated. Two solid-state airborne radar systems using the In P IMPATT diode are presented and explained.

#### REFERENCES

- [1] H.A.El-Motaafy, "Full-scale computer simulation of TRAPATT diodes," The Third National Radio Science Conference, Cairo 1985

- [2] H.El-Motaafy " A New Physical Explantation for the High-Efficiency Mode of Operation of Ga As IMPATT Diodes.",Seventh Conference on Solid-State Symposium ,Cairo April,1984
- [3] H.A.El-Motaafy,"The Modes of Operations of Ga As IMPATT Diode,"The Third National Radio Symposium Conference ,Cairo 1985

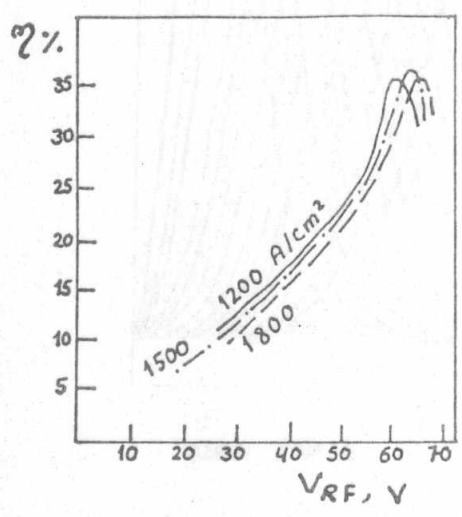


FIG.1-THE EFFECIENCY VERSUS Vrf (F=14 G HZ)

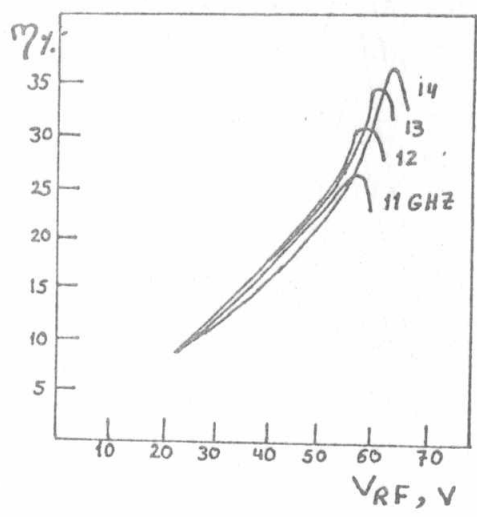


FIG.2-THE EFFECIENCY VERSUS Vrf (Jdc=1500 A/cm )

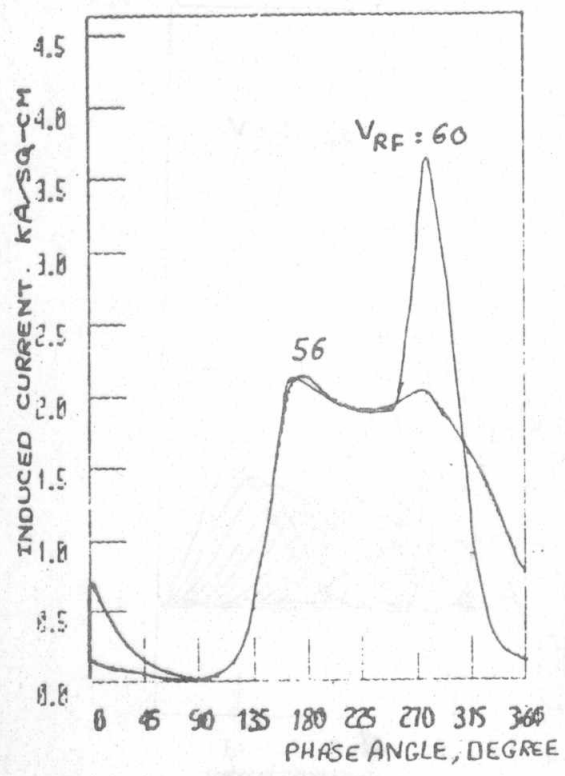
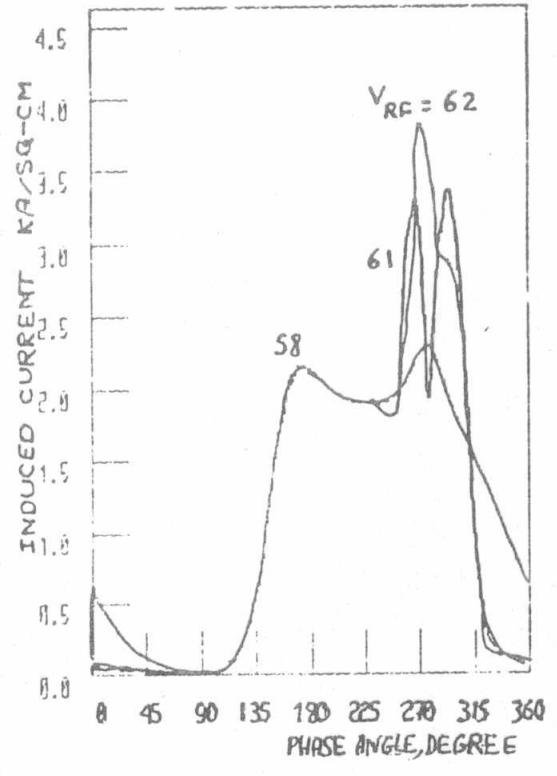


FIG.3-THE INDUCED CURRENT AT F=14 G HZ AND Jdc=1200 A/cm



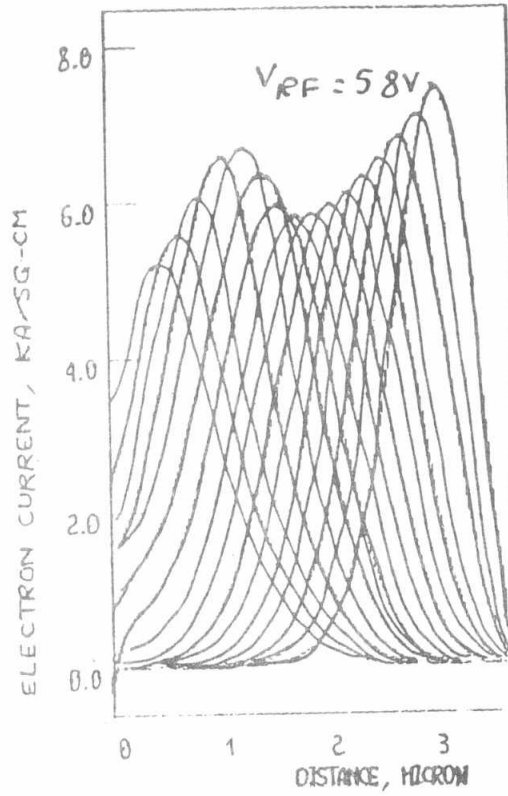
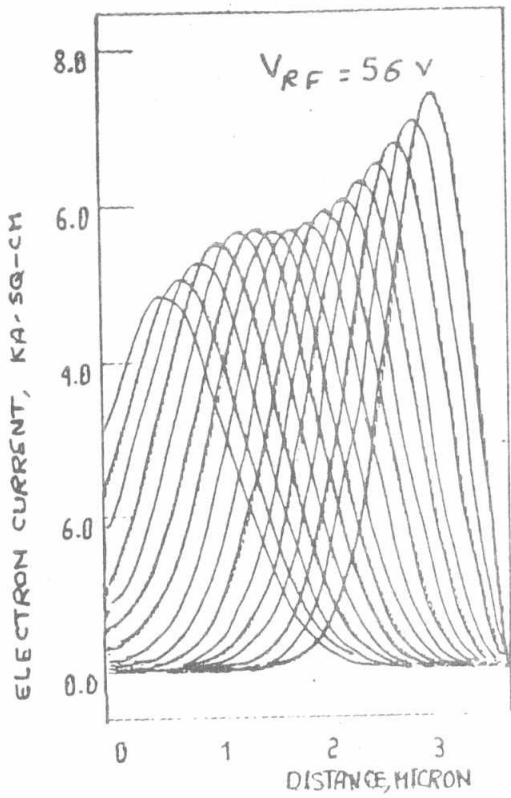


FIG.4.a--THE SPATIAL DISTRIBUTION OF THE ELECTRON CURRENT ( $J_{dc}=1200 \text{ A/cm}^2$ )

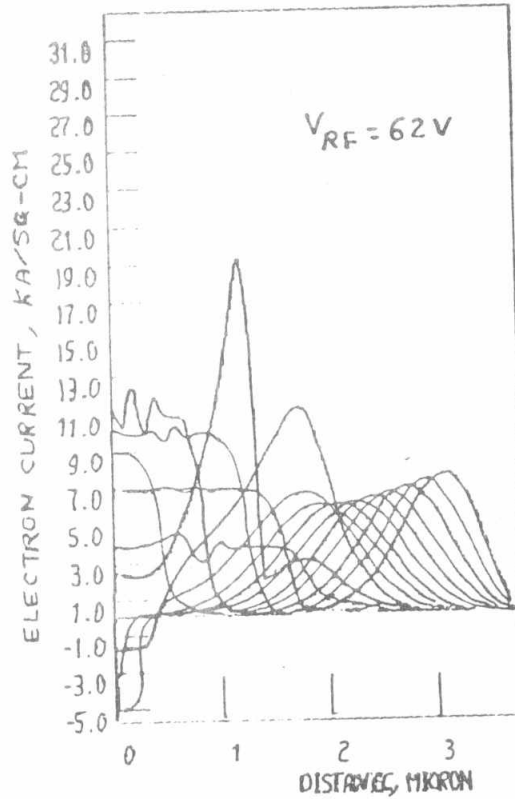
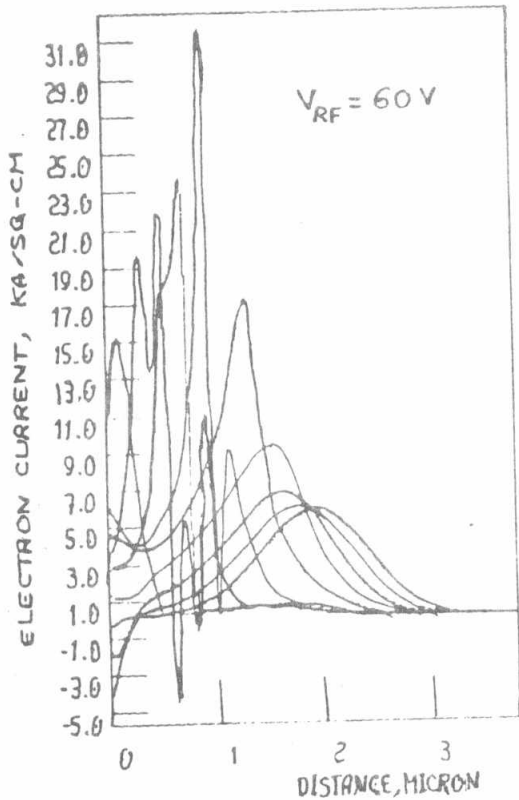


FIG.4.b--THE SPATIAL DISTRIBUTION OF THE ELECTRON CURRENT ( $F=14 \text{ G HZ}, J_{dc}=1200 \text{ A/cm}^2$ )

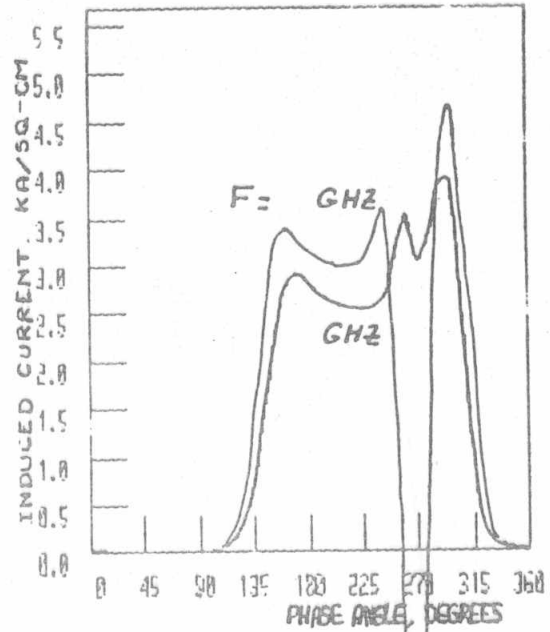
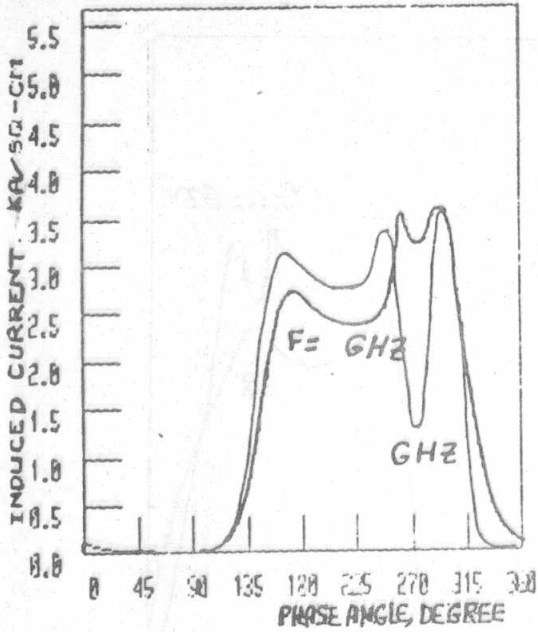


FIG.5-THE INDUCED CURRENT AT  $J_{dc}=1500 \text{ A/cm}^2$   
AND  $V_{rf}=62 \text{ V}$

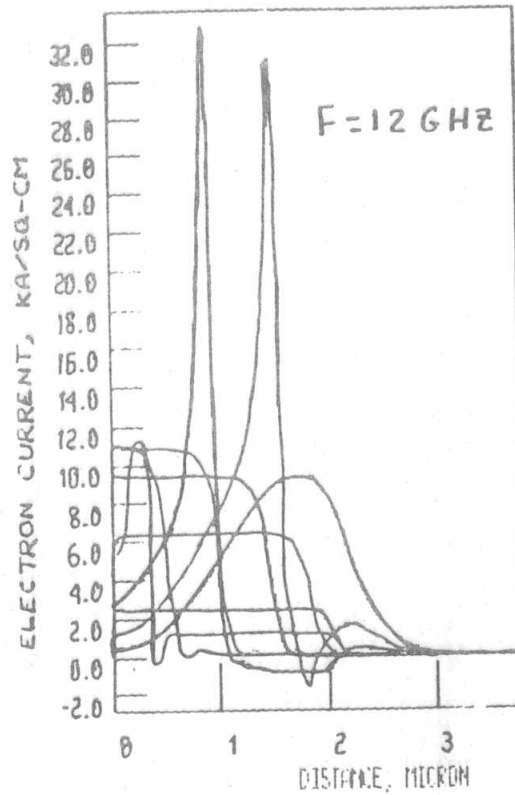
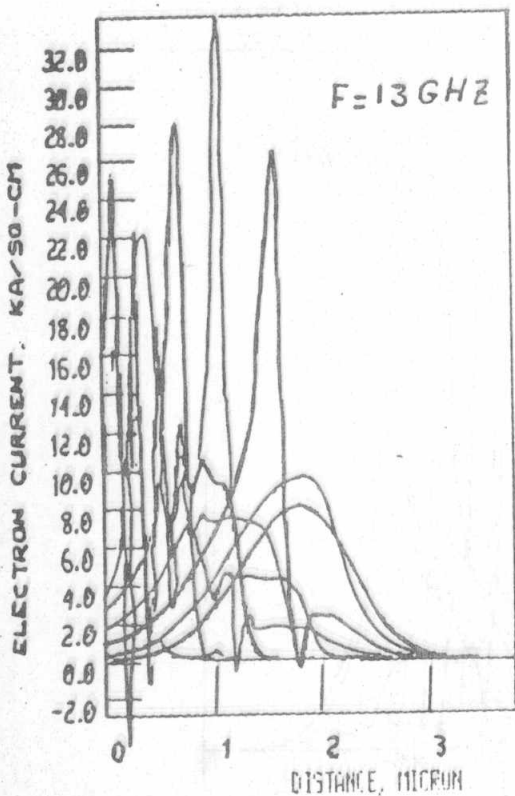


FIG.6-THE SPATIAL DISTRIBUTION OF THE  
ELECTRON CURRENT AT  $V_{rf}=62 \text{ V}$

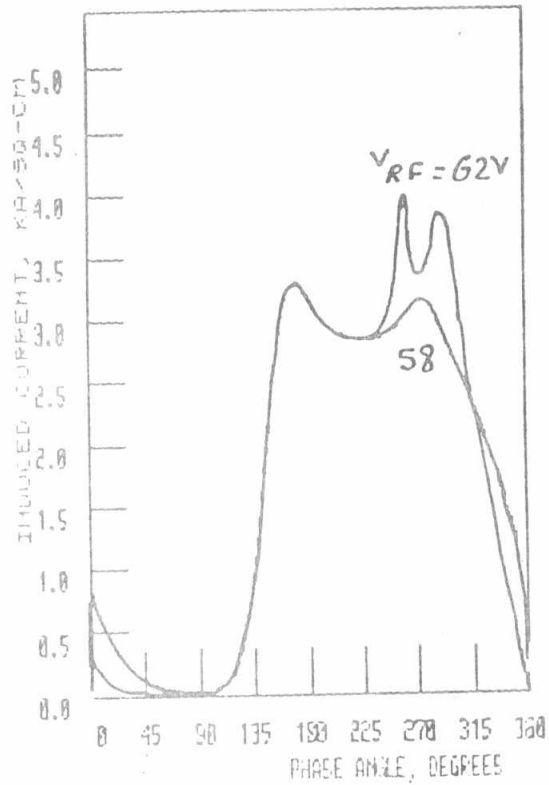
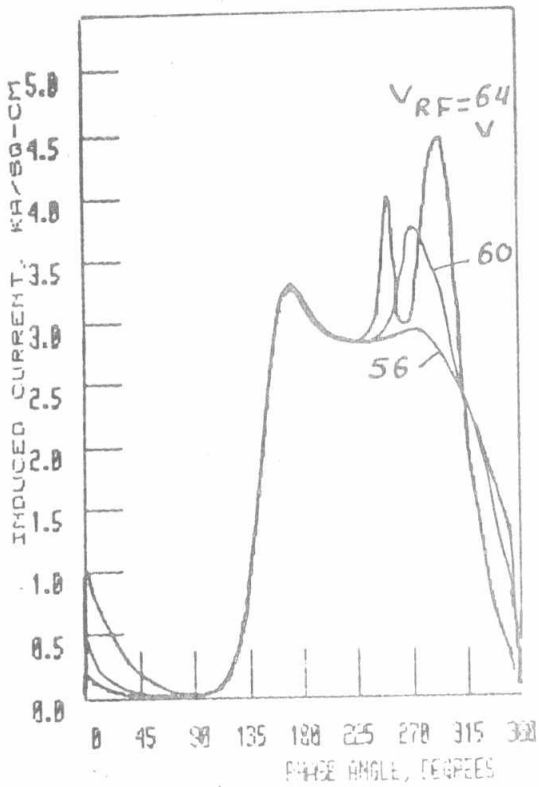


FIG.7-THE INDUCED CURRENT AT  $J_{dc}=1800 \text{ A/cm}^2$

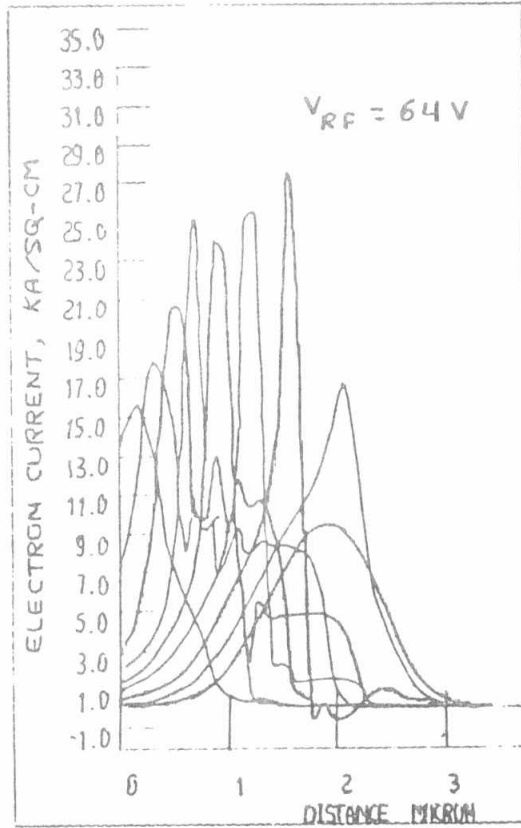
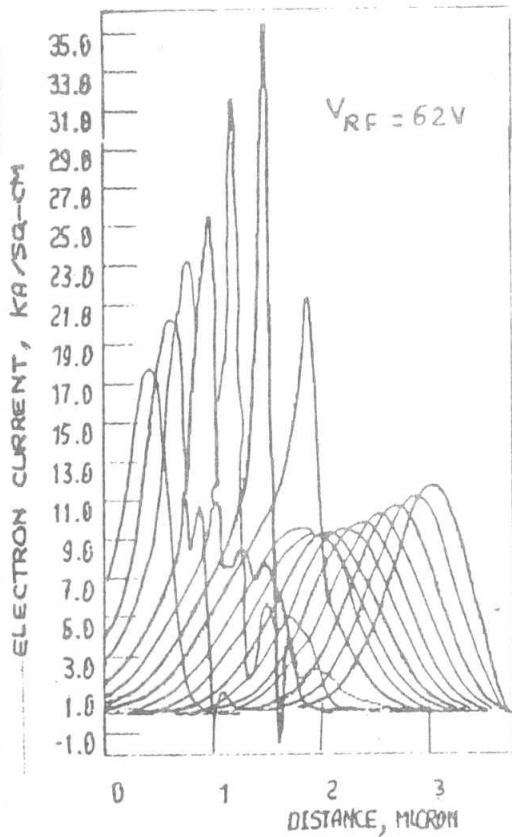


FIG.8-THE SPATIAL DISTRIBUTION OF THE ELECTRON CURRENT AT  $F=14 \text{ G HZ}$  AND  $J_{dc}=1800 \text{ A/cm}^2$



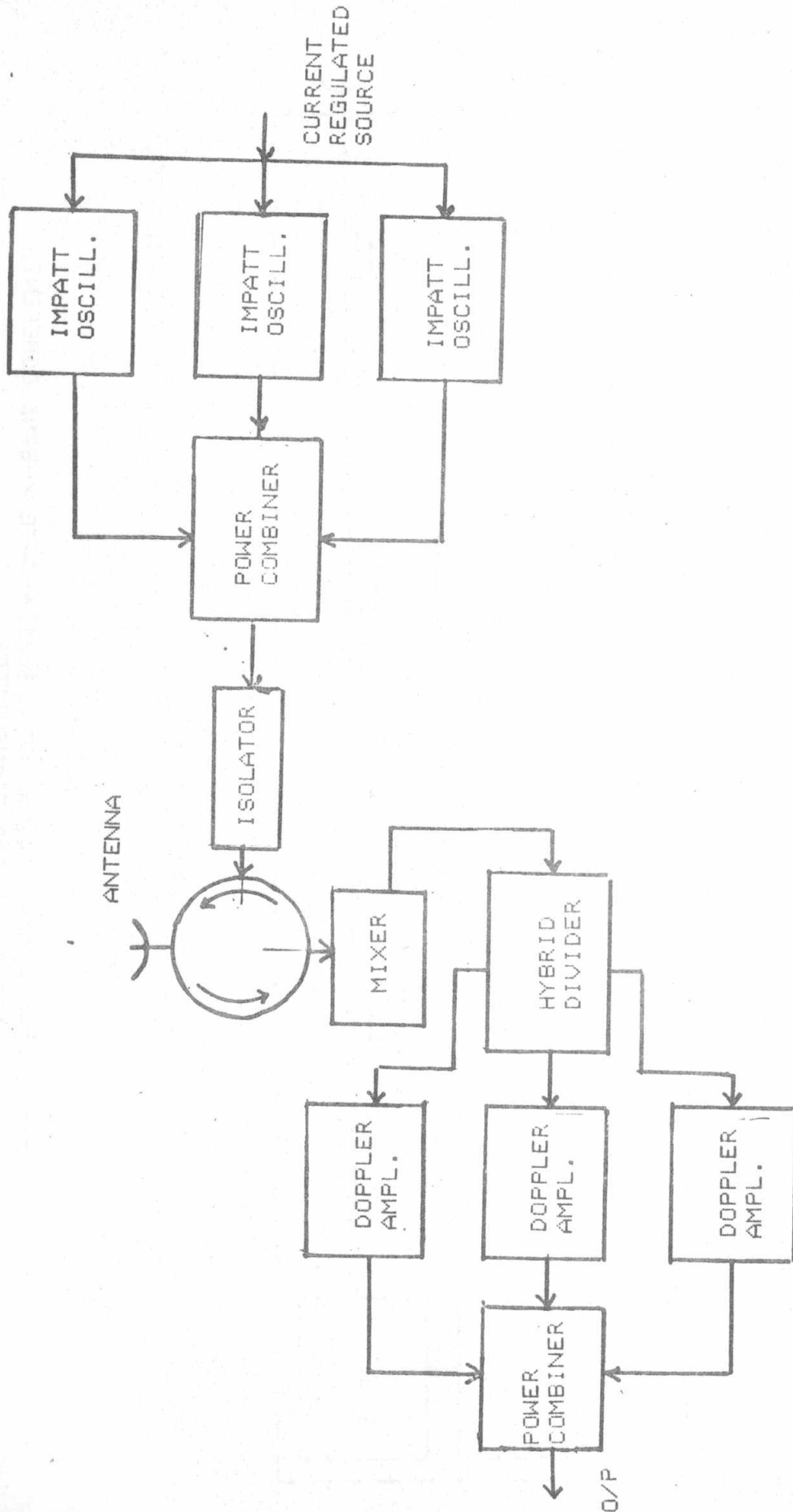


FIG.9-THE BLOCK DIAGRAM OF A SOLID-STATE X-BAND DOPPLER RADAR.

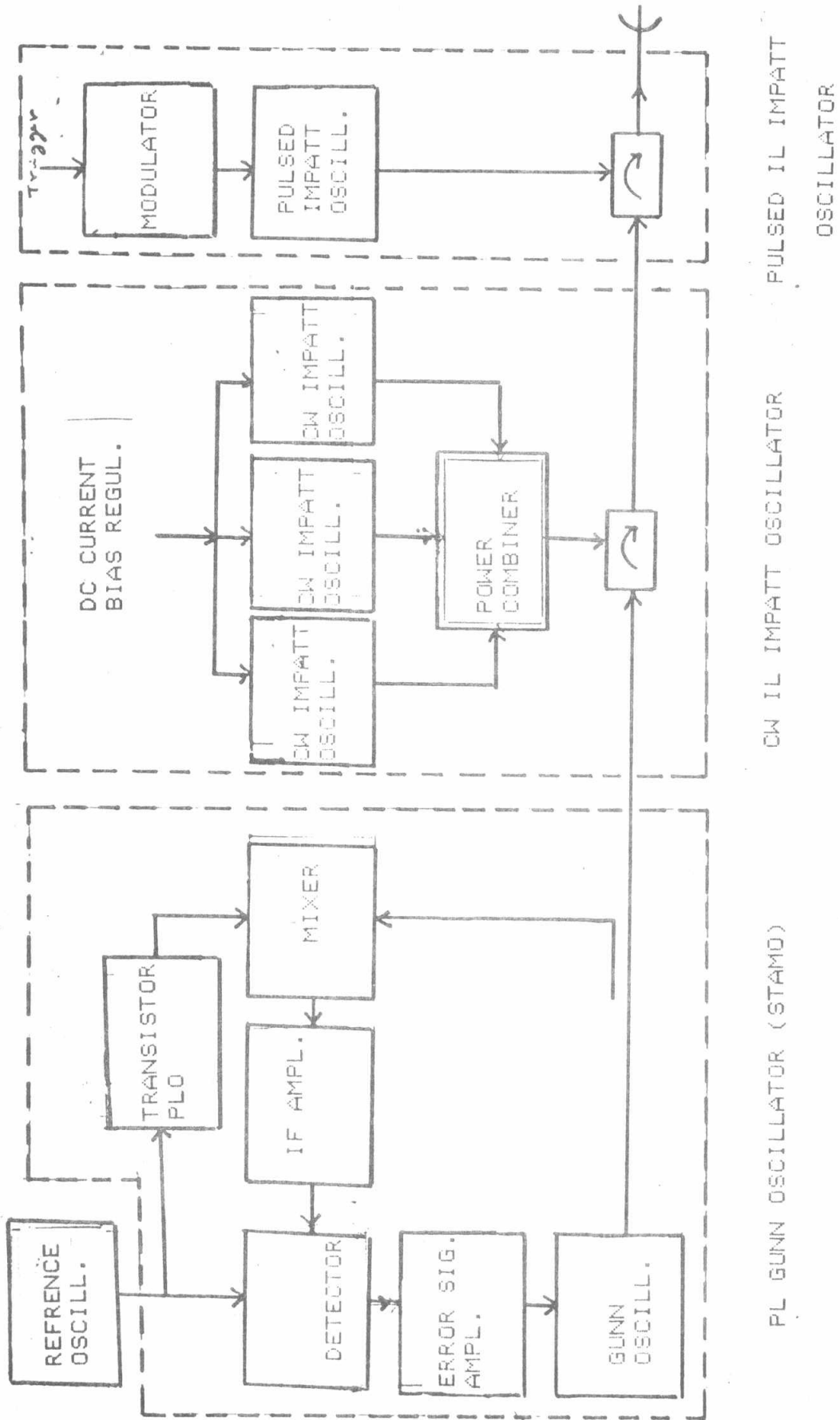


FIG.10-THE BLOCK DIAGRAM OF A SOLID-STATE X-BAND COHERENT AIRBORNE RADAR TRANSMITTER.